



A Characterization of Low Luminance Static and Dynamic Modulation Transfer Function Curves for P-1, P-43, and P-53 Phosphors

By

Howard H. Beasley
John S. Martin
Victor Klymenko
Thomas H. Harding
Robert W. Verona



UES, Incorporated

and

Clarence E. Rash

Aircrew Health and Performance Division

July 1995

19950905 037

Approved for public release; distribution unlimited.

**U.S. Army Aeromedical Research Laboratory
Fort Rucker, Alabama 36362-0577**

Notice

Qualified requesters

Qualified requesters may obtain copies from the Defense Technical Information Center (DTIC), Cameron Station, Alexandria, Virginia 22314. Orders will be expedited if placed through the librarian or other person designated to request documents from DTIC.

Change of address

Organizations receiving reports from the U.S. Army Aeromedical Research Laboratory on automatic mailing lists should confirm correct address when corresponding about laboratory reports.

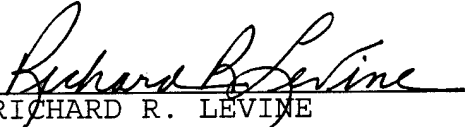
Disposition

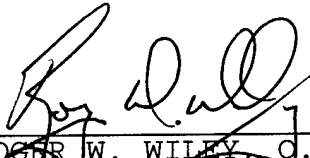
Destroy this document when it is no longer needed. Do not return it to the originator.

Disclaimer

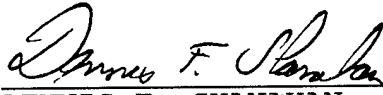
The views, opinions, and/or findings contained in this report are those of the author(s) and should not be construed as an official Department of the Army position, policy, or decision, unless so designated by other official documentation. Citation of trade names in this report does not constitute an official Department of the Army endorsement or approval of the use of such commercial items.

Reviewed:


RICHARD R. LEVINE
LTC, MS
Director, Aircrew Health and Performance Division


ROGER W. WILEY, O. D., Ph.D.
Chairman, Scientific
Review Committee

Released for publication:


DENNIS F. SHANAHAN
Colonel, MC, SFS
Commanding

REPORT DOCUMENTATION PAGE

Form Approved
OMB No. 0704-0188

1a. REPORT SECURITY CLASSIFICATION Unclassified			1b. RESTRICTIVE MARKINGS		
2a. SECURITY CLASSIFICATION AUTHORITY			3. DISTRIBUTION / AVAILABILITY OF REPORT Approved for public release; distribution unlimited		
2b. DECLASSIFICATION / DOWNGRADING SCHEDULE					
4. PERFORMING ORGANIZATION REPORT NUMBER(S) USAARL Report No. 95-29			5. MONITORING ORGANIZATION REPORT NUMBER(S)		
6a. NAME OF PERFORMING ORGANIZATION U.S. Army Aeromedical Research Laboratory		6b. OFFICE SYMBOL (If applicable) SGRD-UAS-VS	7a. NAME OF MONITORING ORGANIZATION U.S. Army Medical Research and Materiel Command		
6c. ADDRESS (City, State, and ZIP Code) P.O. Box 620577 Fort Rucker, AL 36362-0577			7b. ADDRESS (City, State, and ZIP Code) Fort Detrick Frederick, MD 21702-5012		
8a. NAME OF FUNDING / SPONSORING ORGANIZATION		8b. OFFICE SYMBOL (If applicable)	9. PROCUREMENT INSTRUMENT IDENTIFICATION NUMBER		
8c. ADDRESS (City, State, and ZIP Code)			10. SOURCE OF FUNDING NUMBERS		
			PROGRAM ELEMENT NO. 0602787A	PROJECT NO. 3E1672 787A879	TASK NO. BG
					WORK UNIT ACCESSION NO. 164
11. TITLE (Include Security Classification) (U) A Characterization of Low Luminance Static and Dynamic Modulation Transfer Function Curves for P-1, P-43, and P-53 Phosphors					
12. PERSONAL AUTHOR(S) Beasley, Howard H., Martin, John S., Klymenko, Victor, Harding, Thomas H., Verona, Robert W., and Rash, Clarence E.,					
13a. TYPE OF REPORT Final		13b. TIME COVERED FROM _____ TO _____		14. DATE OF REPORT (Year, Month, Day) 1995 July	
				15. PAGE COUNT 17	
16. SUPPLEMENTARY NOTATION					
17. COSATI CODES			18. SUBJECT TERMS (Continue on reverse if necessary and identify by block number)		
FIELD	GROUP	SUB-GROUP			
20	06				
23	02				
19. ABSTRACT (Continue on reverse if necessary and identify by block number)					
<p>A counterphase modulation technique is used to measure the static and dynamic modulation transfer functions for three phosphors of current interest to U.S. Army aviation helmet-mounted displays (P-1, P-43, and P-53).</p> <p>A family of modulation transfer curves, one for each temporal frequency, is presented for each phosphor. The measured MFT curves generally support the supposition that phosphor persistence is a critical parameter in the ability of a CRT display to accurately reproduce contrast modulation transfer in dynamic environments.</p>					
20. DISTRIBUTION / AVAILABILITY OF ABSTRACT <input checked="" type="checkbox"/> UNCLASSIFIED/UNLIMITED <input type="checkbox"/> SAME AS RPT. <input type="checkbox"/> DTIC USERS			21. ABSTRACT SECURITY CLASSIFICATION Unclassified		
22a. NAME OF RESPONSIBLE INDIVIDUAL Chief, Scientific Support Center			22b. TELEPHONE (Include Area Code) 334-255-6907		22c. OFFICE SYMBOL MCMR-UAX-SI

Table of contents

	Page
List of figures	1
List of tables	2
Acknowledgments	3
Introduction	5
Methodology	6
Test displays	6
Instrumentation	8
Display setup	9
Procedure	10
Results and discussion	11
References	16
Appendix A - List of equipment manufacturers	17

List of figures

Figure no.	Page
1. Typical modulation transfer function curve	7
2. Miniature cathode ray tube	7
3. Pictorial diagram of the measurement setup	8
4. Modulation transfer curves for P-1	11
5. Modulation transfer curves for P-43	12
6. Modulation transfer curves for P-53, low luminance	12

List of figures (Continued)

7. Modulation transfer curves for P-53, high luminance . .	13
8. A comparison of modulation transfer function curves for 0 Hz	14
9. A comparison of modulation transfer function curves for 10 Hz	14

List of tables

	Page
1. Phosphor characteristics	6
2. Spatial and temporal frequencies	9

Accession For	
NTIS CRA&I	<input checked="" type="checkbox"/>
DTIC TAB	<input type="checkbox"/>
Unannounced	<input type="checkbox"/>
Justification	
By	
Distribution/	
Availability Codes	
Dist	Avail and/or Special
A-1	

Acknowledgments

The authors wish to thank Mr. Udo Volker Nowak and Ms. Gloria Kennedy for their editorial review.

The miniature cathode ray tubes used in this evaluation were supplied by Honeywell, Inc., Military Avionics Division, St. Louis Park, Minnesota, under the auspices of Cooperative Research and Development Agreement DAMD17-93-0742.

This work is supported by the U.S. Army Medical Research and Development Command under Contract No. DAMD17-91-C-1081.

=====
This page intentionally left blank.
=====

Introduction

A number of different types of displays are used in various military applications. Currently, most of these displays are based on cathode ray tubes (CRTs), which use the cathodoluminescence process of phosphors to produce the display images. To ensure faithful reproduction of scenes on the displays, it is desirable to characterize a display's ability to perform this function. As argued by Rash and Verona (1987) and Verona et al. (1994), characterization must assess both the static and dynamic performance of the display.

Using contrast as the primary attribute of a scene, the modulation transfer function (MTF) is a standard metric used to evaluate display performance. Contrast, generally defined as a measure of the difference between the brightest and darkest regions of a scene, can be expressed in a number of ways. For CRT displays, modulation contrast, or Michelson contrast, often is considered an appropriate metric for describing the display's capacity to convey relative luminance (Task, 1979). Based on a sinusoidal input, modulation contrast (M_c), is defined as

$$M_c = (L_{\max} - L_{\min}) / (L_{\max} + L_{\min}),$$

where L_{\max} is the maximum luminance and L_{\min} is the minimum luminance. Modulation contrast can be related to the integer number of gray scales that an analog display is capable of reproducing.

The capacity of a display to reproduce contrast is spatial and temporal frequency dependent. Spatial frequency refers to the rate of luminance change over space, typically expressed for a display as the number of cycles per millimeter (mm) of display width. Temporal frequency refers to the rate of luminance change over time, which is expressed in Hertz. Temporal frequencies can be related to rates of motion within a scene or between the scene and sensor. Generally, modulation contrast values are measured for a specific display and for a selected temporal frequency. When expressed as ratios to the input modulation and plotted as a function of spatial frequency, the resulting curve (Figure 1) is referred to as the display's modulation transfer function (MTF) for the selected temporal frequency. For a static CRT image, the MTF can be interpreted as the MTF for the condition where the relative motion within the scene is zero. It has become customary to use the term dynamic MTF for temporal frequencies greater than zero.

In this evaluation, the static and dynamic MTFs of three phosphors were measured: P-1, P-43, and P-53. Table 1 provides a brief summary of each phosphor's characteristics. P-1 and P-43 are phosphors associated with the Integrated Helmet and Display

Sighting System (IHADSS) helmet-mounted display (HMD) used in the AH-64 Apache helicopter. (Note: P-1 was the phosphor selected originally for use in the IHADSS. This phosphor was replaced later by P-43. The replacement was prompted by image smearing which contributed to a flight mishap and was the result of the temporal characteristics of the P-1 phosphor.) P-53 is under consideration for use in the RAH-66 Comanche HMD, the Helmet Integrated Display Sight Subsystem (HIDSS).

For the purpose of this evaluation, the important difference between the phosphors is their persistence. Persistence is defined as the time required for the intensity to decay to some percentage of its maximum value following excitation. The 10 percent point is typically used. Table 1 shows the persistence values (10%) to be 1.2, 6.7, and 24 milliseconds (ms) for P-43, P-53, and P-1, respectively.

Table 1.

Phosphor characteristics

Phosphor number	Color	Range (nanometers)	Class	Persistence (10%)
1	Yellow-green	492 to 577	Medium	24.0 ms
43	Yellow-green	451 to 560	Medium-short	1.2 ms
53	Yellow-green	405 to 695	Medium	6.7 ms

Methodology

The instrumentation and procedures for measuring both the static and dynamic contrast modulation values were basically the same. Measurements were performed using the sinusoidal counter-phase modulation technique described in Verona et al., 1994.

Test displays

The displays evaluated were miniature 1-inch diameter CRTs (Figure 2). A single display was evaluated for each of the three phosphors. The CRTs were supplied by Honeywell, Inc.* The P-43 CRT was a production line IHADSS CRT. The P-1 and P-53 tubes were research and development test CRTs.

* See Appendix A.

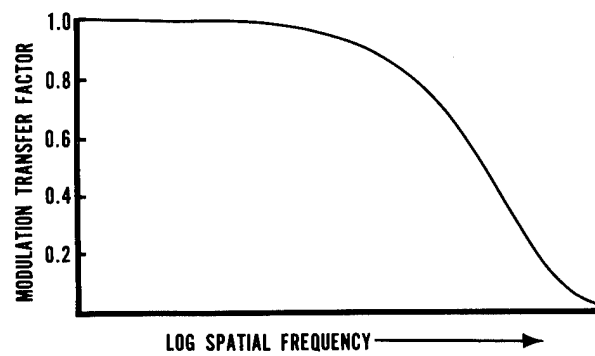


Figure 1. Typical modulation transfer function curve.

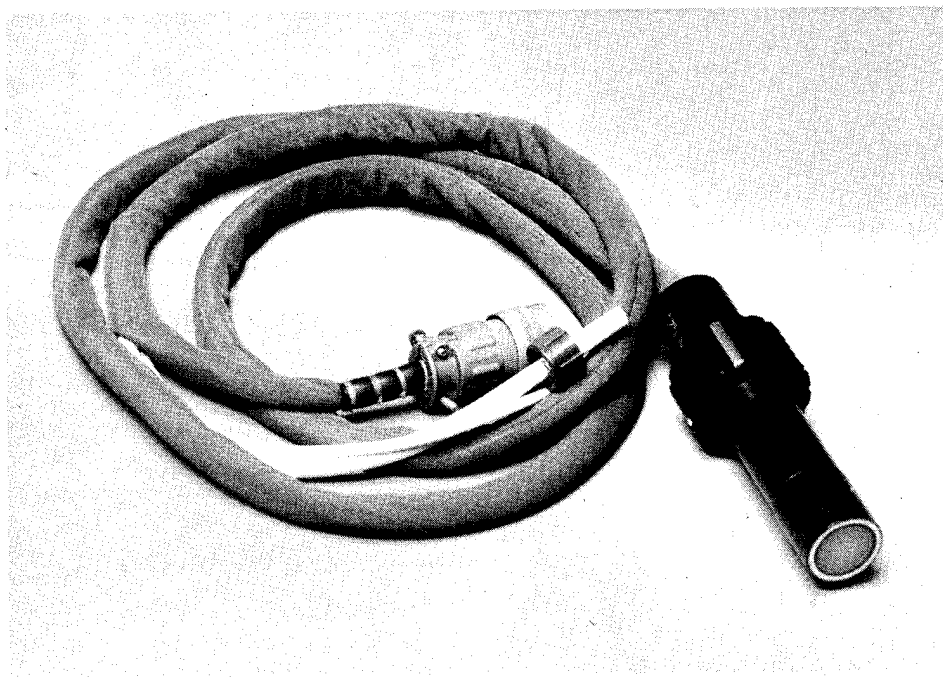


Figure 2. Miniature cathode ray tube.

Instrumentation

A pictorial diagram of the experimental setup is presented in Figure 3. Stimulus patterns were generated with a Hewlett-Packard* model HP-98731 Turbo-SRX computer graphics workstation. The output of the computer was fed to a Folsom Research, Inc.* model 8910 color graphics converter which produced a RS-170A NTSC video signal. This video signal was used to drive the display under evaluation. The software which produced the stimulus patterns was written in the C programming language running in a UNIX environment. Except for aliasing effects, the patterns theoretically could be generated at any desired spatial frequency and presented at any temporal frequency at or below 30 Hertz. For the evaluation presented here, combinations of the spatial and temporal frequencies presented in Table 2 were used.

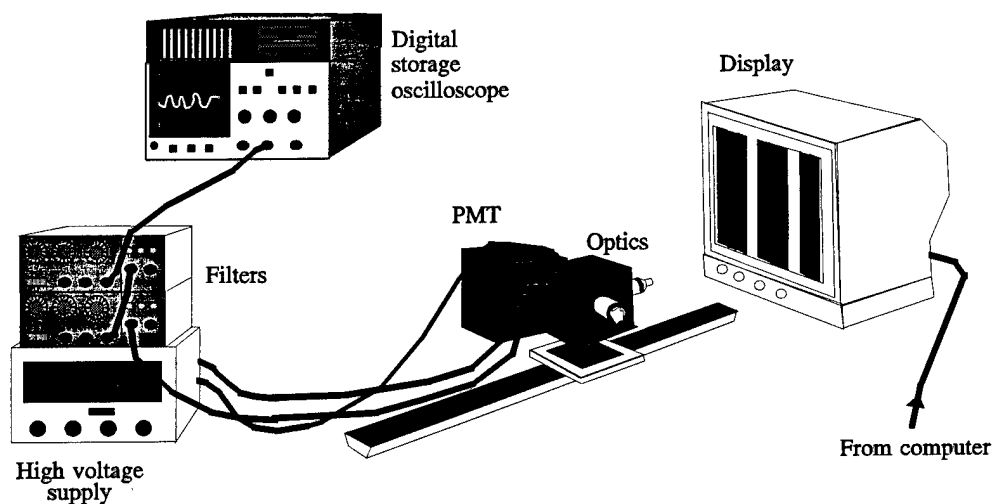


Figure 3. Pictorial diagram of the experimental setup.

An EG&G Gamma Scientific, Inc.* model DR-2 digital radiometer, model D-46A photomultiplier tube (PMT) assembly with 4 MHz high frequency amplifier, and model 700-10 photometric microscope (5X) with a 25 X 8000 micron slit were used as an effective photometer to convert the spatial and temporal luminance values into an electrical signal which was measured using a Tektronix* model 2440 digital storage oscilloscope. The model DR-2 radiometer was used only as a source of high voltage

Table 2.

Spatial and temporal frequencies

Spatial (Cycles/millimeters)	Temporal (Hertz)
0.2, 0.4, 0.6, 0.8, 1.0, 1.3, 1.7, 1.9, 2.1, 2.5, 3.8, 4.2, 5.0, 6.2, 7.5, 8.4, 9.4, 10.5	0, 1.875, 3.75, 5.0, 7.5, 10.0

for the PMT. A high voltage value of 700 volts was used. The output of the high frequency amplifier of the PMT was filtered by two Frequency Devices, Inc.*, model 901F electronic filters before being fed to the oscilloscope. The filters, connected in series, acted as a low pass filter with a cutoff frequency of 35 Hertz and provided 40 dB of gain. The temporal response of the photometer is very critical for the dynamic measurements. The limited range of response speeds typically encountered in off-the-shelf photometers is inadequate for reliable dynamic measurements; therefore, the video or high frequency output of the photometer was used. The electronic filters provided amplification and filtered out high frequency noise, improving the signal-to-noise ratio. The output of the filter was displayed on a digital storage oscilloscope.

Display setup

Each phosphor was characterized for operating parameter values which equated to night viewing conditions. For the simulated night environment, a value of 15 footlamberts was chosen. Using a white/black ratio of 100:1, this required the black level luminance to be 0.15 footlambert. Following adjustment of focus and aspect ratio using the manufacturer's recommended procedures, the display's brightness and contrast were set using the following procedure.

Brightness and contrast controls were adjusted to their minimum settings (fully counterclockwise). Inputting a low spatial frequency square wave 1-volt peak-to-peak video signal (RS-170A, NTSC 525-line rate), the brightness control was increased until the raster barely was visible. The contrast control then was advanced to a setting which produced a 15-footlambert luminance value at the peak of the pattern (maximum video level). The black level luminance (minimum video level) was examined to see if the 0.15-footlambert value was present.

As required, the brightness and contrast controls were adjusted, alternately, to achieve the 100:1 ratio. For each display, the minimum and maximum luminance values were verified to be 0.15 and 15 footlamberts, respectively, using an EG&G model 3100 photometric system.

In addition to the low luminance measurement for the three phosphors, the P-53 phosphor also was evaluated for a representative high output luminance. This additional evaluation was performed because the P-53 phosphor is the proposed phosphor for use in the RAH-66 Comanche helmet-mounted-display, the Helmet Integrated Display Sight Subsystem. This system currently has relay optics based on a low efficiency catadioptric design. To compensate for this low throughput, the CRT may be required to operate at the high end of its luminance range. To investigate the impact of this possibility on the phosphor's MTF, an additional measurement was performed with the P-53 peak luminance set to 309.7 footlamberts. With the contrast maximized for best picture, the black level luminance was measured to be 7.3 footlamberts, producing a white/black ratio of approximately 42:1.

Procedure

The evaluation was performed in a fully darkened laboratory. The test displays were driven by computer generated static and dynamic vertical sine wave spatial patterns, i.e., the long dimension of the pattern at a 90° angle (vertical) to the display's scan line structure.

To evaluate the static case, zero Hertz temporal frequency, contrast measurements were made over the spatial frequency range of approximately three cycles per display width (0.2 cycles/mm) to the cutoff frequency, where the modulation contrast approached zero. For each spatial frequency, a peak of the sine wave was positioned in front of the photometer and the resulting maximum output was read from the display of the oscilloscope and recorded; then a trough of the sine wave was positioned and the resulting minimum output was read and recorded. These data, when used to calculate the contrast values, represent the sine wave response of the display for the static image condition.

For the dynamic case, the spatial sine wave patterns also were modulated temporally at selected sinusoidal frequencies. One temporal cycle of the stimulus consisted of the luminance at a position on the display changing from its brightest value to its darkest value and back to its brightest value (counterphase). The luminance variations on the display were sinusoidal in both spatial and temporal domains.

The first nonzero temporal frequency was selected and the appropriate input signal was applied to the display at each spatial frequency. For each spatial frequency, the photometer output signal was acquired using the oscilloscope. From the digitized waveform, the peak and trough values were obtained and used to calculate the modulation contrast value. This procedure was repeated for each temporal frequency.

Modulation transfer ratios were calculated from the input and output modulation contrast data for all spatial and temporal frequency combinations and presented as MTF curves. The input contrast modulation values were obtained by inputting each spatial and temporal frequency combination signal to the oscilloscope and reading the respective peak and trough values.

Results and discussion

Families of MTF curves for the P-1, P-43, P-53 (low and high luminance) phosphors are presented in Figures 4-7, respectively. Each family consists of six MTF curves, one for each temporal

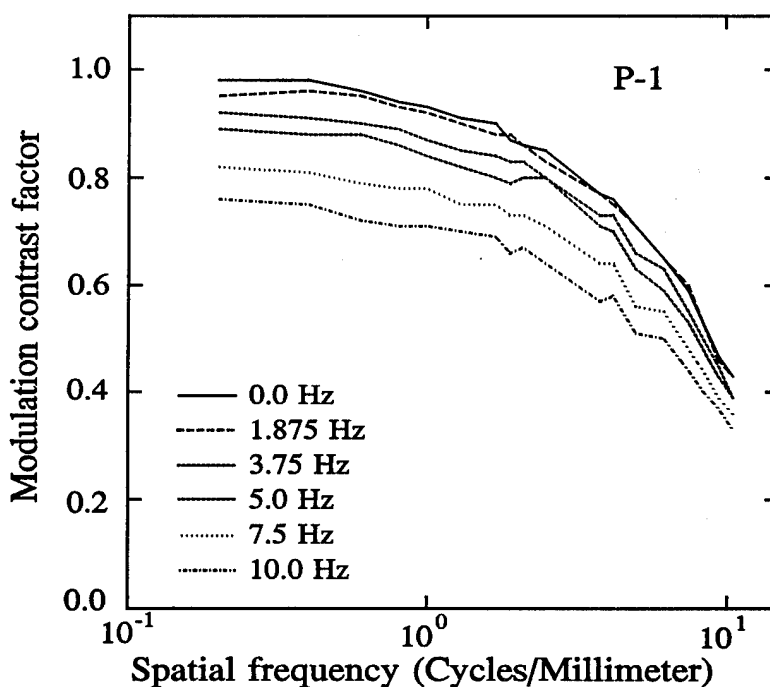


Figure 4. Modulation transfer function curves for P-1 phosphor display.

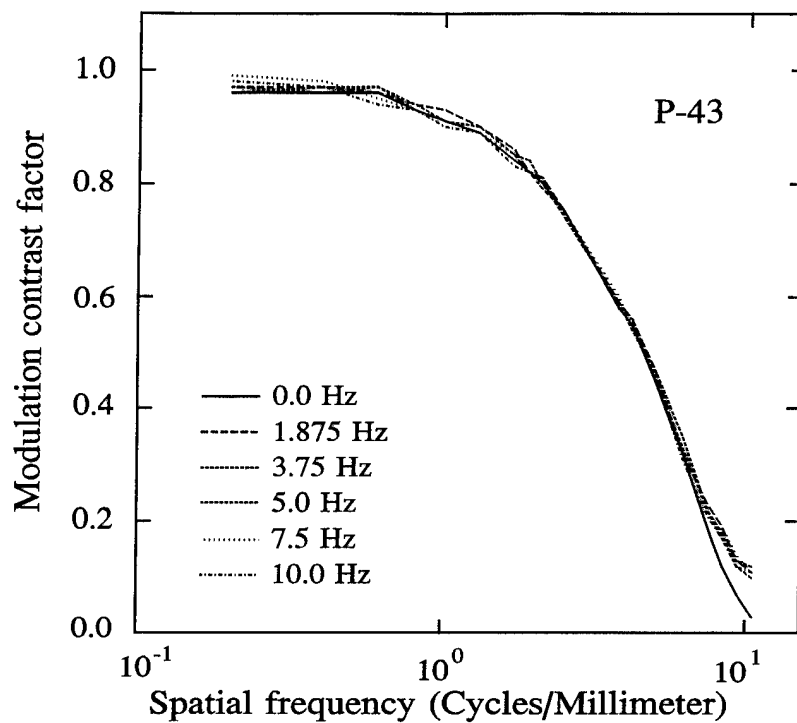


Figure 5. Modulation transfer function curves for P-43 phosphor display.

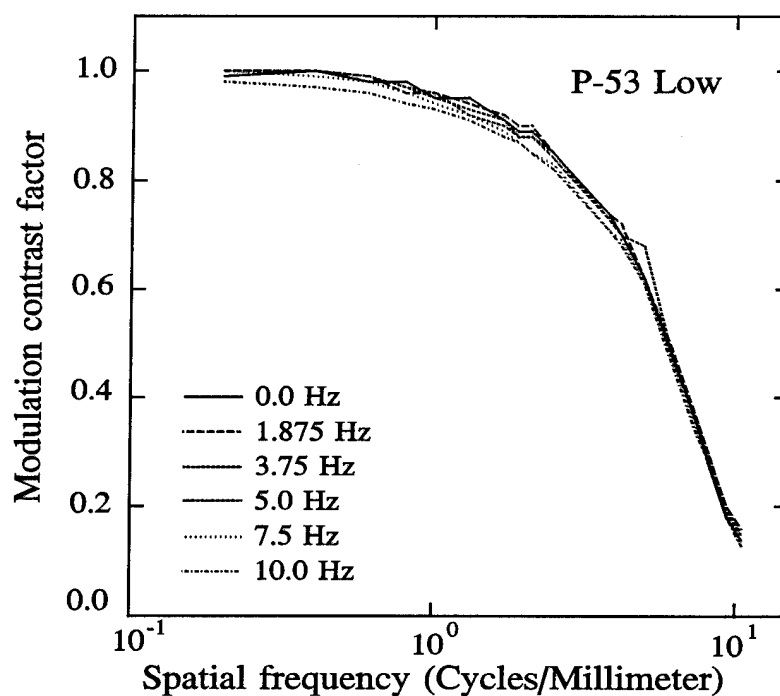


Figure 6. Modulation transfer function curves for P-53 phosphor display at low luminance.

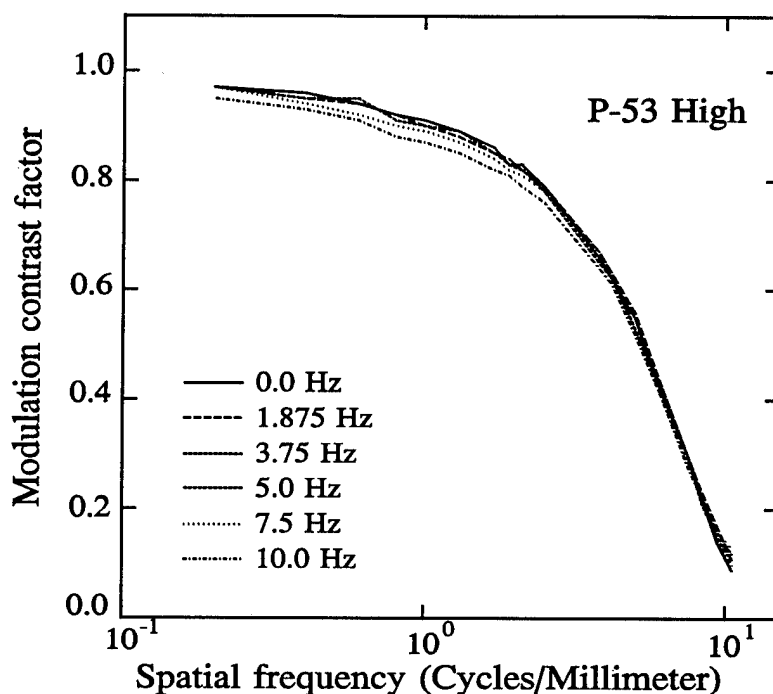


Figure 7. Modulation transfer function curves for P-53 phosphor display at high luminance.

frequency. Graphs comparing the 0 Hz and 10 Hz MTF curves for all of the phosphors (and conditions) are presented in Figures 8 and 9, respectively.

The P-43 curves (Figure 5) do not appear to show any differences for the various temporal frequencies. This is expected due to the relatively short P-43 persistence value of 1.2 ms. P-53, with the somewhat longer persistence value of 6.7 ms, appears to show a loss of modulation transfer at 10 Hz for the low luminance condition (Figure 6). For the P-53 high luminance condition (Figure 7), the data suggest the MTF curves for both the 7.5 and 10 Hz temporal frequencies demonstrate reductions. This additional fall off for 7.5 Hz most likely is due to blooming resulting from the higher luminance. The curves for the P-1 phosphor (Figure 4) with its 24 ms persistence appear to show distinct differences between each temporal frequency.

In Figures 8 and 9, the modulation transfer function curves are compared for the 0 and 10 Hz temporal frequencies, respectively. The most obvious feature of these comparisons is the crossover of the MTF curve of the P-1 phosphor. The significance of this crossover is a greater contrast modulation transfer at the higher spatial frequencies for the P-1 phosphor

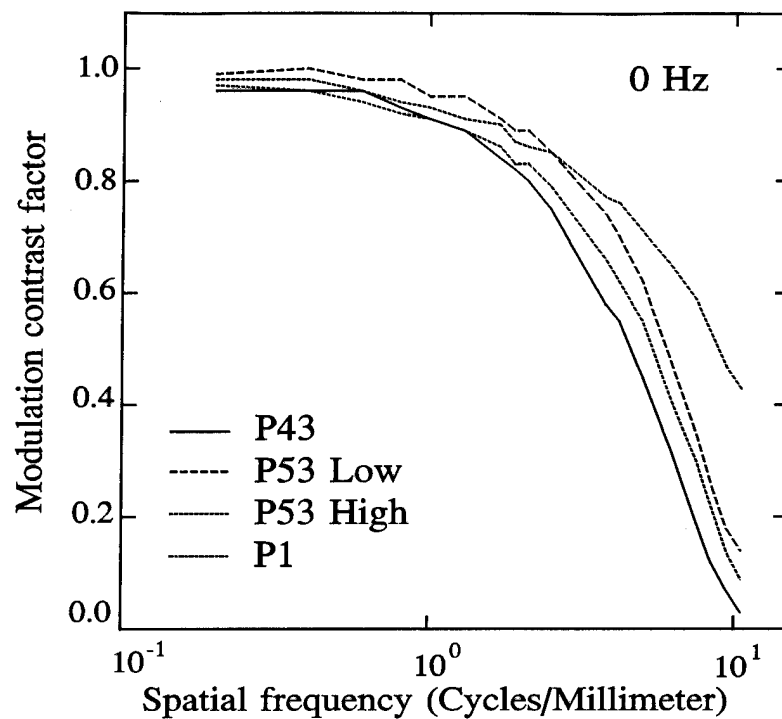


Figure 8. A comparison of modulation transfer function curves for 0 Hz.

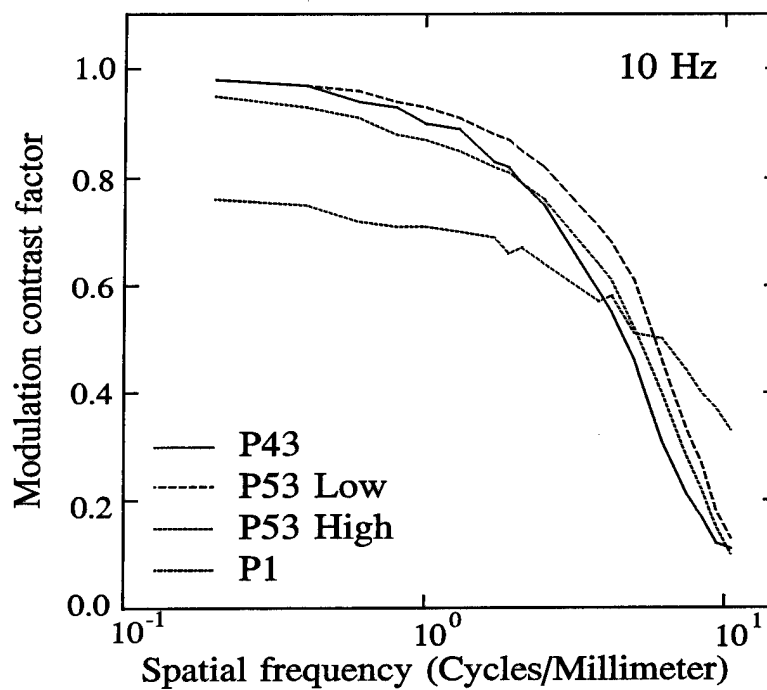


Figure 9. A comparison of modulation transfer function curves for 10 Hz.

over the other phosphors. While the cause of this phenomenon is debatable, it is thought to be based on the particulate size of the phosphor material. In other words, it is suspected that the P-1 phosphor has smaller particulate size, thereby increasing its higher spatial frequency response.

In summary, the family of MTF curves measured for each phosphor generally supports the supposition that phosphor persistence is a critical parameter in the ability of a CRT display to accurately reproduce contrast modulation transfer in dynamic environments.

References

- Rash, C. E., and Verona, R. W. 1987. "Temporal aspects of electro-optical imaging systems," Imaging Sensors and Displays, Proceedings SPIE, Vol. 765, pp. 22-25.
- Task, H. L. 1979. An evaluation and comparison of several measures of image quality for television displays. Wright-Patterson Air Force Base, OH: Aerospace Medical Research Laboratory, AMRL TR-79-7-9.
- Verona, R. W., Beasley, H. H., Martin, J. S., Klymenko, V., and Rash, C. E. 1994. Dynamic sine wave response measurements of CRT displays using sinusoidal counterphase modulation. Fort Rucker, AL: U.S. Army Aeromedical Research Laboratory. USAARL Report No. 94-22.

Appendix A.

List of equipment manufacturers

EG&G Gamma Scientific, Inc.
3777 Ruffin Road
San Diego, CA 92123

Frequency Devices, Inc.
25 locust Street
Haverhill, MA 01830

Folsom Research, Inc.
526 E. Bidwell Street
Folsom, CA 95630

Hewlett-Packard Co.
4700 Bayou Blvd.
Pensacola, FL 32503

Honeywell, Inc
1625 Zarthan Ave.
St. Louis Park, MN 55416

Tektronix, Inc.
P.O. Box 500
Beaverton, OR 97077

Initial distribution

Commander, U.S. Army Natick Research,
Development and Engineering Center
ATTN: SATNC-MIL (Documents
Librarian)
Natick, MA 01760-5040

Library
Naval Submarine Medical Research Lab
Box 900, Naval Sub Base
Groton, CT 06349-5900

Chairman
National Transportation Safety Board
800 Independence Avenue, S.W.
Washington, DC 20594

Executive Director, U.S. Army Human
Research and Engineering Directorate
ATTN: Technical Library
Aberdeen Proving Ground, MD 21005

Commander
10th Medical Laboratory
ATTN: Audiologist
APO New York 09180

Commander
Man-Machine Integration System
Code 602
Naval Air Development Center
Warminster, PA 18974

Naval Air Development Center
Technical Information Division
Technical Support Detachment
Warminster, PA 18974

Commander
Naval Air Development Center
ATTN: Code 602-B
Warminster, PA 18974

Commanding Officer, Naval Medical
Research and Development Command
National Naval Medical Center
Bethesda, MD 20814-5044

Commanding Officer
Armstrong Laboratory
Wright-Patterson
Air Force Base, OH 45433-6573

Deputy Director, Defense Research
and Engineering
ATTN: Military Assistant
for Medical and Life Sciences
Washington, DC 20301-3080

Director
Army Audiology and Speech Center
Walter Reed Army Medical Center
Washington, DC 20307-5001

Commander, U.S. Army Research
Institute of Environmental Medicine
Natick, MA 01760

Commander/Director
U.S. Army Combat Surveillance
and Target Acquisition Lab
ATTN: SFAE-IEW-JS
Fort Monmouth, NJ 07703-5305

Director
Federal Aviation Administration
FAA Technical Center
Atlantic City, NJ 08405

Commander, U.S. Army Test
and Evaluation Command
Directorate for Test and Evaluation
ATTN: AMSTE-TA-M (Human Factors
Group)
Aberdeen Proving Ground,
MD 21005-5055

Naval Air Systems Command
Technical Air Library 950D
Room 278, Jefferson Plaza II
Department of the Navy
Washington, DC 20361

Director
U.S. Army Ballistic
Research Laboratory
ATTN: DRXBR-OD-ST Tech Reports
Aberdeen Proving Ground, MD 21005

Commander
U.S. Army Medical Research
Institute of Chemical Defense
ATTN: SGRD-UV-AO
Aberdeen Proving Ground,
MD 21010-5425

Commander
USAMRDALC
ATTN: SGRD-RMS
Fort Detrick, Frederick, MD 21702-5012

Director
Walter Reed Army Institute of Research
Washington, DC 20307-5100

HQ DA (DASG-PSP-O)
5109 Leesburg Pike
Falls Church, VA 22041-3258

Harry Diamond Laboratories
ATTN: Technical Information Branch
2800 Powder Mill Road
Adelphi, MD 20783-1197

U.S. Army Materiel Systems
Analysis Agency
ATTN: AMXSY-PA (Reports Processing)
Aberdeen Proving Ground
MD 21005-5071

U.S. Army Ordnance Center
and School Library
Simpson Hall, Building 3071
Aberdeen Proving Ground, MD 21005

U.S. Army Environmental
Hygiene Agency
ATTN: HSHB-MO-A
Aberdeen Proving Ground, MD 21010

Technical Library Chemical Research
and Development Center
Aberdeen Proving Ground, MD
21010-5423

Commander
U.S. Army Medical Research
Institute of Infectious Disease
ATTN: SGRD-UIZ-C
Fort Detrick, Frederick, MD 21702

Director, Biological
Sciences Division
Office of Naval Research
600 North Quincy Street
Arlington, VA 22217

Commandant
U.S. Army Aviation
Logistics School ATTN: ATSQ-TDN
Fort Eustis, VA 23604

Headquarters (ATMD)
U.S. Army Training
and Doctrine Command
ATTN: ATBO-M
Fort Monroe, VA 23651

IAF Liaison Officer for Safety
USAF Safety Agency/SEFF
9750 Avenue G, SE
Kirtland Air Force Base
NM 87117-5671

Naval Aerospace Medical
Institute Library
Building 1953, Code 03L
Pensacola, FL 32508-5600

Command Surgeon
HQ USCENTCOM (CCSG)
U.S. Central Command
MacDill Air Force Base, FL 33608

Director
Directorate of Combat Developments
ATTN: ATZQ-CD
Building 515
Fort Rucker, AL 36362

U.S. Air Force Institute
of Technology (AFIT/LDEE)
Building 640, Area B
Wright-Patterson
Air Force Base, OH 45433

Henry L. Taylor
Director, Institute of Aviation
University of Illinois-Willard Airport
Savoy, IL 61874

Chief, National Guard Bureau
ATTN: NGB-ARS
Arlington Hall Station
111 South George Mason Drive
Arlington, VA 22204-1382

Commander
U.S. Army Aviation and Troop Command
ATTN: AMSAT-R-ES
4300 Goodfellow Bouvelard
St. Louis, MO 63120-1798

U.S. Army Aviation and Troop Command
Library and Information Center Branch
ATTN: AMSAV-DIL
4300 Goodfellow Boulevard
St. Louis, MO 63120

Federal Aviation Administration
Civil Aeromedical Institute
Library AAM-400A
P.O. Box 25082
Oklahoma City, OK 73125

Commander
U.S. Army Medical Department
and School
ATTN: Library
Fort Sam Houston, TX 78234

Commander
U.S. Army Institute of Surgical Research
ATTN: SGRD-USM
Fort Sam Houston, TX 78234-6200

AAMRL/HEX
Wright-Patterson
Air Force Base, OH 45433

Air University Library
(AUL/LSE)
Maxwell Air Force Base, AL 36112

Product Manager
Aviation Life Support Equipment
ATTN: SFAE-AV-LSE
4300 Goodfellow Boulevard
St. Louis, MO 63120-1798

Commander and Director
USAE Waterways Experiment Station
ATTN: CEWES-IM-MI-R,
CD Department
3909 Halls Ferry Road
Vicksburg, MS 39180-6199

Commanding Officer
Naval Biodynamics Laboratory
P.O. Box 24907
New Orleans, LA 70189-0407

Assistant Commandant
U.S. Army Field Artillery School
ATTN: Morris Swott Technical Library
Fort Sill, OK 73503-0312

Mr. Peter Seib
Human Engineering Crew Station
Box 266
Westland Helicopters Limited
Yeovil, Somerset BA20 2YB UK

U.S. Army Dugway Proving Ground
Technical Library, Building 5330
Dugway, UT 84022

U.S. Army Yuma Proving Ground
Technical Library
Yuma, AZ 85364

AFFTC Technical Library
6510 TW/TSTL
Edwards Air Force Base,
CA 93523-5000

Commander
Code 3431
Naval Weapons Center
China Lake, CA 93555

Aeromechanics Laboratory
U.S. Army Research and Technical Labs
Ames Research Center, M/S 215-1
Moffett Field, CA 94035

Sixth U.S. Army
ATTN: SMA
Presidio of San Francisco, CA 94129

Commander
U.S. Army Aeromedical Center
Fort Rucker, AL 36362

Strughold Aeromedical Library
Document Service Section
2511 Kennedy Circle
Brooks Air Force Base, TX 78235-5122

Dr. Diane Damos
Department of Human Factors
ISSM, USC
Los Angeles, CA 90089-0021

U.S. Army White Sands
Missile Range
ATTN: STEWS-IM-ST
White Sands Missile Range, NM 88002

U.S. Army Aviation Engineering
Flight Activity
ATTN: SAVTE-M (Tech Lib) Stop 217
Edwards Air Force Base, CA 93523-5000

Ms. Sandra G. Hart
Ames Research Center
MS 262-3
Moffett Field, CA 94035

Commander
USAMRDALC
ATTN: SGRD-UMZ
Fort Detrick, Frederick, MD 21702-5009

Commander
U.S. Army Health Services Command
ATTN: HSOP-SO
Fort Sam Houston, TX 78234-6000

U. S. Army Research Institute
Aviation R&D Activity
ATTN: PERI-IR
Fort Rucker, AL 36362

Commander
U.S. Army Safety Center
Fort Rucker, AL 36362

U.S. Army Aircraft Development
Test Activity
ATTN: STEBG-MP-P
Cairns Army Air Field
Fort Rucker, AL 36362

Commander
USAMRDALC
ATTN: SGRD-PLC (COL R. Gifford)
Fort Detrick, Frederick, MD 21702

TRADOC Aviation LO
Unit 21551, Box A-209-A
APO AE 09777

Netherlands Army Liaison Office
Building 602
Fort Rucker, AL 36362

British Army Liaison Office
Building 602
Fort Rucker, AL 36362

Italian Army Liaison Office
Building 602
Fort Rucker, AL 36362

Directorate of Training Development
Building 502
Fort Rucker, AL 36362

Chief
USAHEL/USAAVNC Field Office
P. O. Box 716
Fort Rucker, AL 36362-5349

Commander, U.S. Army Aviation Center
and Fort Rucker
ATTN: ATZQ-CG
Fort Rucker, AL 36362

Chief
Test & Evaluation Coordinating Board
Cairns Army Air Field
Fort Rucker, AL 36362

Canadian Army Liaison Office
Building 602
Fort Rucker, AL 36362

German Army Liaison Office
Building 602
Fort Rucker, AL 36362

French Army Liaison Office
USAAVNC (Building 602)
Fort Rucker, AL 36362-5021

Australian Army Liaison Office
Building 602
Fort Rucker, AL 36362

Dr. Garrison Rapmund
6 Burning Tree Court
Bethesda, MD 20817

Commandant, Royal Air Force
Institute of Aviation Medicine
Farnborough, Hampshire GU14 6SZ UK

Defense Technical Information
Cameron Station, Building 5
Alexandra, VA 22304-6145

Commander, U.S. Army Foreign Science
and Technology Center
AIFRTA (Davis)
220 7th Street, NE
Charlottesville, VA 22901-5396

Commander
Applied Technology Laboratory
USARTL-ATCOM
ATTN: Library, Building 401
Fort Eustis, VA 23604

Commander, U.S. Air Force
Development Test Center
101 West D Avenue, Suite 117
Eglin Air Force Base, FL 32542-5495

Aviation Medicine Clinic
TMC #22, SAAF
Fort Bragg, NC 28305

Dr. H. Dix Christensen
Bio-Medical Science Building, Room 753
Post Office Box 26901
Oklahoma City, OK 73190

Commander, U.S. Army Missile
Command
Redstone Scientific Information Center
ATTN: AMSMI-RD-CS-R
/ILL Documents
Redstone Arsenal, AL 35898

Director
Army Personnel Research Establishment
Farnborough, Hants GU14 6SZ UK

U.S. Army Research and Technology
Laboratories (AVSCOM)
Propulsion Laboratory MS 302-2
NASA Lewis Research Center
Cleveland, OH 44135

Commander
USAMRDALC
ATTN: SGRD-ZC (COL John F. Glenn)
Fort Detrick, Frederick, MD 21702-5012

Dr. Eugene S. Channing
166 Baughman's Lane
Frederick, MD 21702-4083

U.S. Army Medical Department
and School
USAMRDALC Liaison
ATTN: HSMC-FR
Fort Sam Houston, TX 78234

Dr. A. Kornfield
895 Head Street
San Francisco, CA 94132-2813

NVESD
AMSEL-RD-NV-ASID-PST
(Attn: Trang Bui)
10221 Burbeck Road
Fort Belvoir, VA 22060-5806

CA Av Med
HQ DAAC
Middle Wallop
Stockbridge, Hants S020 8DY UK

Dr. Christine Schlichting
Behavioral Sciences Department
Box 900, NAVUBASE NLON
Groton, CT 06349-5900

Aerospace Medicine Team
HQ ACC/SGST3
162 Dodd Boulevard, Suite 100
Langley Air Force Base,
VA 23665-1995

Commander
Aviation Applied Technology Directorate
ATTN: AMSAT-R-TV
Fort Eustis, VA 23604-5577

COL Yehezkel G. Caine, MD
Surgeon General, Israel Air Force
Aeromedical Center Library
P. O. Box 02166 I.D.F.
Israel

HQ ACC/DOHP
205 Dodd Boulevard, Suite 101
Langley Air Force Base,
VA 23665-2789

41st Rescue Squadron
41st RQS/SG
940 Range Road
Patrick Air Force Base,
FL 32925-5001

48th Rescue Squadron
48th RQS/SG
801 Dezonias Road
Holloman Air Force Base,
NM 88330-7715

35th Fighter Wing
35th FW/SG
PSC 1013
APO AE 09725-2055

66th Rescue Squadron
66th RQS/SG
4345 Tyndall Avenue
Nellis Air Force Base, NV 89191-6076

71st Rescue Squadron
71st RQS/SG
1139 Redstone Road
Patrick Air Force Base,
FL 32925-5000

Director
Aviation Research, Development
and Engineering Center
ATTN: AMSAT-R-Z
4300 Goodfellow Boulevard
St. Louis, MO 63120-1798

Commander
USAMRDALC
ATTN: SGRD-ZB (COL C. Fred Tyner)
Fort Detrick, Frederick, MD 21702-5012

Commandant
U.S. Army Command and General Staff
College
ATTN: ATZL-SWS-L
Fort Leavenworth, KS 66027-6900